

Folding and Unfolding of Human Lactoferrin at Interfaces: Expected X-ray Reflectivity Profiles

Yohko F. Yano

Synchrotron Life Science Center, Ritsumeikan University, 1-1-1, Noji-higashi, Kusatsu, Shiga, 565-8577

Fax: 81-77-561-2680, e-mail: y-yano@fc.ritsumei.ac.jp

X-ray reflectivity profiles of human lactoferrin adsorbed at water interfaces have been calculated using the structure determined by neutron reflection measurements [Lu *et al.*, *Langmuir*, **21**, 3354 (2005)]. A significant difference in the expected profiles was observed between the folding and the unfolding lactoferrin at the interfaces. Time-resolved X-ray reflectivity measurements for probing the protein unfolding dynamics are proposed.

Key words: X-ray reflection, neutron reflection, protein folding, interface

1. INTRODUCTION

Details of protein structures determined from X-ray and NMR studies indicate the importance of understanding how proteins fold into three-dimensional structures. However, protein folding is not well understood and remains a central question in biochemistry. Small-angle X-ray scattering (SAXS) technique is a powerful tool for characterizing folding dynamics [1]. But the random orientation of proteins in water limits the amount of structural information this technique can provide.

Since proteins fold their hydrophobic regions within hydrophilic regions in water, conformational changes would be expected when they adsorb at water interfaces. Only a few studies report direct measurements of protein conformational changes upon adsorption at air/water or solid/water interfaces [2]. Lu *et al.* observed strong structural unfolding of human lactoferrin at the air/water interface by neutron reflectivity (NR) [3]. From neutron or X-ray reflectivity (XR) data, the structural information along to the surface normal can be derived more precisely than that derived from SAXS.

In the present study, expected X-ray reflectivity profiles for 'unfolded' human lactoferrin at the air/water have been calculated using the previous neutron reflectivity study done by Lu *et al.* [3]. These are compared with the profile for 'folded' human lactoferrin predicted from the structure in water by exploiting the potential of time-resolved X-ray reflection technique for probing protein folding dynamics.

Since the X-ray reflection geometry for air-water interfaces is restricted by the liquid free surface, limited beam lines are available for the surface horizontal geometry at synchrotron facilities in Japan. Therefore, examining the measurements without a need for the surface horizontal geometry at solid/liquid interfaces is worthwhile.

Recently, several reports on X-ray investigation of solid/liquid interfaces using high-energy synchrotron radiation have been released. Miller *et al.* investigated biological systems using 18 keV X-rays [4]. They measured the reflectivity from biological membranes formed on single crystal quartz substrates at the

CMC-CAT beam line at the APS synchrotron source. Their scan up to $q_z = 0.5 \text{ \AA}^{-1}$ covering 8 orders in the dynamic range of intensity was completed in 30 min.

2. ANALYTICAL METHODS

2.1 Crystalline structure of human lactoferrin

Lactoferrin is a member of the family of iron-binding proteins. It is a homomeric glycoprotein with 700 amino acid residues and a molecular weight of $75 - 80 \times 10^3$. It is bilobal in structure with symmetrical halves (Fig.1). Peptide fragmentation and X-ray studies [5] have shown that the polypeptide chain can be cleaved into two nearly equal lobes, each carrying one iron-binding site. Each lobe is an ellipsoid with approximate dimensions of $55 \times 35 \times 35 \text{ \AA}^3$. The two lobes are connected by an α -helical connection, with the long axes roughly antiparallel. The volume of the protein was estimated by adding the volume of all individual peptides giving a total of $93,600 \text{ \AA}^3$ [3].

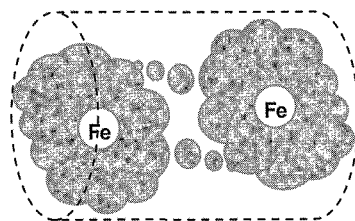


Fig.1 Schematic structure of diferic human lactoferrin

2.2 X-ray reflection geometry

Figure 2 shows a schematic of human lactoferrin (hereafter, HL) at interfaces. An X-ray beam of wavelength λ with wave vector \mathbf{k}_{in} is incident under angle θ with respect to the surface, and the specularly reflected beam leaves the surface with wave vector \mathbf{k}_{out} ($|\mathbf{k}_{in}| = |\mathbf{k}_{out}| = 2\pi/\lambda$). For the solid/water interface shown in Fig. 2(b), it is assumed that the X-ray beam penetrating the water is reflected by the solid/water interface. It is convenient to use the wavevector transfer

$|\mathbf{q}_z| = |\mathbf{k}_{\text{out}} - \mathbf{k}_{\text{in}}| = (4\pi/\lambda)\sin\theta$ as the independent variable rather than θ . Since q_z is always parallel to the surface normal, one can evaluate the electron density profile to the surface normal from the q_z dependence of reflected beam intensities. The electron density profile and electron density of the bulk liquid are denoted $\rho(z)$ and ρ_{bulk} , respectively. X-ray reflectivity $R(q_z)$ is defined as the reflected beam intensities normalized by the incident beam intensities.

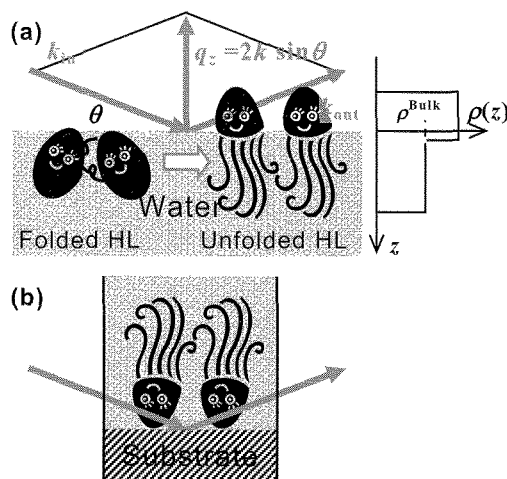


Fig. 2 Schematic of HL at (a) an air/water interface and (b) solid/water interface along with a diagram of the basic principle of the measurement.

2.3 Models of folded and unfolded human lactoferrin at the air/water interface

Lu *et al.* observed that unfolded HL at the air/water interface has two distinct regions, a dense top layer of 15-20 Å on the air side and a diffuse bottom layer extending 50 Å into the aqueous subphase like a jellyfish as shown in Fig. 2. To calculate expected XR profiles based on their results, the electron density profiles of HL at the air/water interface are needed. In the reference 3 (hereafter, Ref. 3), the layer thickness L_i and volume fraction of HL $\varphi_{p,i}$ for each layer ($i = 1$ or 2) are shown. The average neutron scattering length density of the layer i was calculated with using the neutron scattering length ρ_p for the protein and ρ_w for water

$$\rho_i = \varphi_{p,i}\rho_p + \varphi_{w,i}\rho_w \quad (1)$$

where the volume fraction of the water $\varphi_{w,i} = 1 - \varphi_{p,i}$.

Without knowing all of the compositions, the electron density cannot be estimated directly from the neutron scattering length. Therefore, the average electron number density of HL is assumed to be $\rho_p = 0.42 \text{ e}/\text{\AA}^3$, which corresponds to the half of the molecular weight of 80×10^3 divided by the total volume of $93,600 \text{ \AA}^3$; while for the aqueous subphase, 0.3M NaCl solution, it is equal to $\rho_w = 0.34 \text{ e}/\text{\AA}^3$. The average electron number densities of layer i also were calculated using Eq. (1).

To examine the potential of time-resolved X-ray reflection technique for studying protein folding dynamics, it is necessary to determine if significant changes can be observed in the XR profiles during protein adsorption. Since the NR measurements reported in Ref. 3 were obtained under equilibrium conditions (30 min after the sample preparation), the initial

conformation of HL adsorbed at the interface is unknown. It is reasonable to assume that HL adsorbed at the interface initially has a folded structure. We assumed, therefore, HL has the same structure as in the bulk solution determined by small-angle neutron scattering [3]. The volume fraction of HL φ_p inside the cylinder with a diameter of 47 Å denoted in Fig. 1 is 0.52 in the presence of 0.3M NaCl. The base of the cylinder was assumed perpendicular to the air/water interface.

2.4 Models of unfolded human lactoferrin at solid/water interfaces

The XR profiles of HL unfolded at solid/water interfaces also were simulated to examine the effect of the electron density contrast between the water and the substrates. Polystyrene (PS) for low contrast and silicon (Si) for high contrast were chosen as the substrates. The configuration of unfolded HL at the interface is shown in Fig. 2(b).

3. RESULTS

3.1 Folded and unfolded HL at the air/water interface

The XR profiles were calculated using the software Parrat32 [6] with the electron density profiles of step functions estimated above. Figure 3 demonstrates the simulated profiles for HL of 0.1g/L in the presence of 0.3M NaCl. A significant difference is observed near $q_z \sim 0.2 \text{ \AA}^{-1}$.

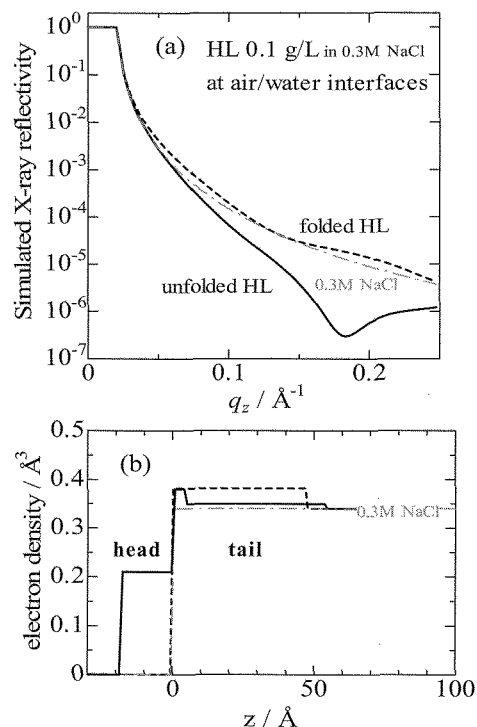


Fig. 3 (a) Simulated X-ray reflectivity profiles of HL at air/water interfaces with the electron density profiles of the step functions represented in (b). Dashed and solid lines indicate the folded and unfolded HL, respectively. The dashed-dotted line represents the Fresnel reflectivity of water subphase with 0.3M NaCl.

3.2 Unfolded HL at solid/water interfaces

The simulated XR profiles of HL at solid/water interfaces are shown in Fig. 4. The corresponding Fresnel reflectivity R_F of the solid/water interfaces are denoted by dashed-dotted lines. A significant difference between the XR profiles with HL and without HL is observed for PS in contrast with Si. However, XR intensity of PS is two orders of magnitude less than that of Si.

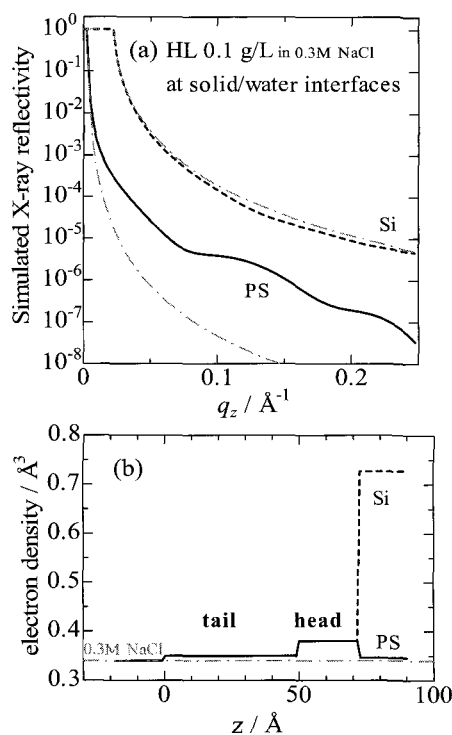


Fig. 4 (a) Simulated X-ray reflectivity profiles of unfolded HL at solid/water interfaces with the density profiles of the step functions represented in (b). Dashed and solid lines indicate the HL adsorbed at the Si or PS surface, respectively. The dashed-dotted lines indicate the corresponding Fresnel reflectivity profiles without HL.

4. DISCUSSIONS

4.1 Origin of the calculated XR profiles

The simulated XR profiles for HL adsorbed at three different hydrophobic interfaces show significant differences despite being assumed to have the same unfolding configuration. To explain such differences, we examined the underlying origin of the calculated XR profile.

The XR profiles are given by:

$$R(q_z) = R_F |\Phi(q_z)|^2 \quad (2)$$

where $|\Phi(q_z)|^2$ is the structure factor along to the surface normal expressed as [7]

$$|\Phi(q_z)|^2 = \left| \frac{1}{\rho^{\text{Bulk}}} \int dz \frac{\partial \langle \rho(z) \rangle}{\partial z} e^{iq_z z} \right|^2 \quad (3)$$

The structure factor of a three layers model with uniform electron density differences, ρ_1, ρ_2, ρ_3 , becomes:

$$\begin{aligned} |\Phi(q_z)|^2 &= \left| \frac{1}{\rho^{\text{Bulk}}} \left\{ \rho_1 + (\rho_2 - \rho_1)e^{iq_z L_1} + (\rho_3 - \rho_2)e^{iq_z L_2} \right\} \right|^2 \\ &= \left(\frac{1}{\rho^{\text{Bulk}}} \right)^2 \left\{ \rho_1^2 + (\rho_2 - \rho_1)^2 + (\rho_3 - \rho_2)^2 \right. \\ &\quad + 2\rho_1(\rho_2 - \rho_1)\cos(q_z L_1) + 2\rho_1(\rho_3 - \rho_2)\cos(q_z L_2) \\ &\quad \left. + 2(\rho_2 - \rho_1)(\rho_3 - \rho_2)\cos[q_z(L_2 - L_1)] \right\}^2 \quad (4) \end{aligned}$$

The values of density relative to that of water – ρ_1 for the HL tail region, ρ_2 for the HL head region and ρ_3 for the substrates – are summarized in Table 1 and schematically plotted in Fig. 5. The value of ρ^{Bulk} corresponds to each value of ρ_3 . The thicknesses of the tail and head regions of HL are $L_1 = 50 \text{ \AA}$ and $L_2 = 22 \text{ \AA}$, respectively.

Table 1 Electron density relative to that of the water for the three interfaces [$e/\text{\AA}^3$]

interface	ρ_1	ρ_2	ρ_3
Si	0.01	0.04	0.38
PS	0.01	0.04	0.006
Air	0.01	-0.13	-0.34

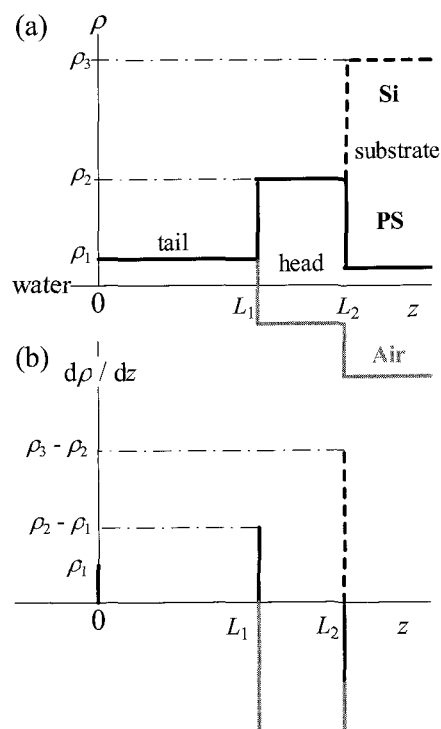


Fig. 5 Schematic density profiles (a) and their derivatives (b) for the three-layer model for three different interfaces.

Figure 6 demonstrates the structure factors calculated by Eq. (4) using the values in Table 1. The absolute value of $|\Phi(q_z)|^2$ is associated with $(1/\rho^{\text{Bulk}})^2$, therefore the largest value is observed for PS. In the case of air, $|\rho_2 - \rho_1| \approx |\rho_3 - \rho_2| \gg |\rho_1|$, the oscillation term

of $(\rho_2 - \rho_1)(\rho_3 - \rho_2)\cos[q_z(L_2 - L_1)]$ in Eq. (4) becomes the main contributor to the structure factor, giving a large dip at $q_z \sim 0.15 \text{ \AA}^{-1}$. In contrast for PS, $|\rho_2 - \rho_1| \approx |\rho_3 - \rho_2| \approx |\rho_1|$, the three oscillation terms equivalently contribute to the $|\Phi(q_z)|^2$, giving more complicated profiles as shown in Fig. 6. For Si, the large density contrast between water and Si gives $|\Phi(q_z)|^2 \approx 1$, which is an XR profile nearly identical to the Fresnel reflectivity of the Si/water interface.

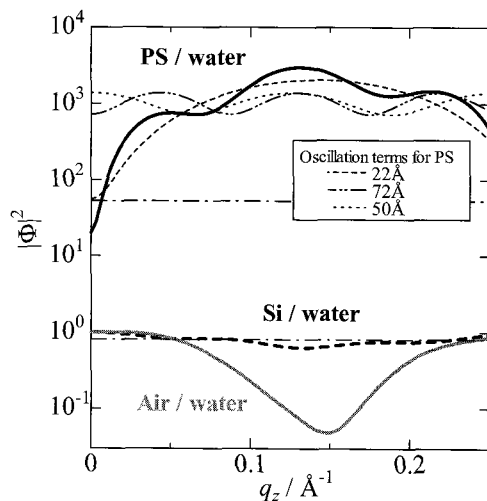


Fig. 6 Structure factors for unfolded HL at several interfaces calculated by Eq. (4). The horizontal dashed-dotted lines are represent the sums of the non-oscillation terms in Eq. (4) and the other broken lines are the three oscillation terms for PS.

4.2 Strategy for time-resolved XR measurements

As shown above, significant differences in the simulated XR profiles in the region of $0.1 < q_z < 0.2 \text{ \AA}^{-1}$ were observed. If the data are taken from the limited q_z region, time-resolved XR measurements within a resolution of 1 min can be easily obtained. Either the angle or energy dispersive method [8] is suitable for the measurements.

Although the surface tension of HL decreases during the first 30 min [3], it is still unclear whether a time resolution of 1 min is sufficient for probing the unfolding process. There are several stages involved in the protein adsorption on the surface: diffusion in the water, adsorption on the surface, unfolding and aggregation with other proteins [9]. Since the folding process in water usually occurs in milliseconds, a time resolution within 1 second might be necessary for probing at the interfaces. Such rapid measurements cannot be performed using the energy dispersive method because of the time resolution limit of available detectors. Repeat of the same process would produce time-resolved XR data with the resolution of millisecond at several fixed angles. A particular flow cell for probing the interface should be developed.

5. CONCLUSIONS

X-ray reflectivity profiles for the unfolded human lactoferrin at several interfaces were calculated based on the results of the neutron reflectivity measurements by Lu *et al.* [3]. At the air/water interface, a significant difference between the folded and unfolded structure is observed near $q_z \sim 0.2 \text{ \AA}^{-1}$, offering the possibility of time-resolved measurements for probing protein dynamics. The calculated XR profile is dominated by the structure of the top layer (hydrophobic region) which is out of the water; while for the polystyrene/water interface, the XR profile is affected by the entire structure of unfolding HL. To obtain the unfolding configuration of proteins more precisely, a substrate with an electron density close to that of water should be chosen.

REFERENCES

- [1] H. Roder, K. Maki and H. Cheng, *Chem. Rev.* **106**, 1836-1861 (2006).
- [2] A. H. Martin, M. B. J. Meinders, M. A. Bos, M. A. C. Stuart and T. Vliet, *Langmuir*, **19**, 2922-2928 (2003).
- [3] J. R. Lu, S. Perumal, X. Zhao, F. Miano, V. Enea, R. R. Heenan and J. Penfold, *Langmuir*, **21**, 3354-3361 (2005).
- [4] C. E. Miller, J. Majewski, T. Gog, and T. L. Kuhl, *Phys. Rev. Lett.* **94**, 238104 (2005).
- [5] See the webpages of Brookhaven Protein Data Bank No. 1b01.
- [6] This Reflectivity software is available from: http://www.hmi.de/bensc/instrumentation/instrumente/v6/refl/parratt_en.htm.
- [7] J. Als-Nielsen and D. McMorrow, "Elements of Modern X-ray Physics", John Wiley & Sons, Ltd (2001) pp.92-98.
- [8] U. Vierl and G. Cevc, *Biochimica et Biophysica Acta* **1325**, 165-177 (1997).
- [9] H. H. J. Jongh, H. A. Kusters, E. Kudryashova, M. B. J. Meinders, D. Trofimova and P. A. Wierenga, *Biopolymers*, **74**, 131-135 (2004).

(Received December 9, 2006; Accepted February 16, 2007)